Image Enhancement

EQ2330 Image and Video Processing, Project 1

Federico Favia
favia@kth.se

Yue Song
yuesong@kth.se

November 19, 2019

Summary

In the project, we investigate some image enhancement and restoration techniques, namely contrast enhancement by histogram equalization, spatial domain smoothing, and image restoration in frequency domain. Both quantitative and qualitative analysis are present in the experimental section.

1 Introduction

As discussed in section 3.3.1 of [1] and course slides [2], the histogram is calculated to show the number of each pixel at with intensity level:

$$p_r = \frac{n_r}{\sum_{j=0}^{L-1} n_j}, \ r = 0, 1, \dots L-1 \tag{1}$$

where L is the number of possible intensity values and n_r denotes the number of pixel with intensity r. The histogram equalization aims at finding a monotonic increasing function which is able to enhance the image contrast. The transform function $T(\cdot)$ can be defined as

$$s = T(r) = round((L-1)\sum_{r=0}^{k} p_r) \tag{2}$$

where r corresponds to intensity level and $round(\cdot)$ indicates rounding to the nearest integer. The new probability distribution $P_s(s)$ can be represented as

$$P_s(s) = P_r(r)|\frac{dr}{ds}| = P_r(r)\frac{dr}{dT(r)} \tag{3}$$

If the intensity level is continuous, we can further get

$$P_s(s) = P_r(r)\frac{dr}{dT(r)} = P_r(r)\frac{dr}{d\ (L-1)\int_0^r p_\omega d\omega} = \frac{1}{L-1} \tag{4}$$

It shows when the intensity is continuous, we will obtain an uniform histogram after equalization. However, intensity levels are discrete in practice, thus this property does not hold.

The image denoising operation is usually done using a filter $h(\cdot)$ by either convolution in spatial domain or multiplication in frequency domain:

$$\begin{aligned} g(x,y) &= f(x,y) \star h(x,y) + \eta(x,y), \\ G(u,v) &= F(u,v) \cdot H(u,v) + N(u,v) \end{aligned} \tag{5}$$

where the lowercase represents the impulse response and uppercase denotes the frequency response. In frequency domain filtering, our task is to find a good estimate of the original image, which balance noise reduction and sharpening of image. A straightforward solution is to use inverse filter:

$$T(u,v) = H^{-1}(u,v) \tag{6}$$

Then the estimate $\hat{F}(u,v)$ is obtained by multiplying $T(u,v)$ with $G(u,v)$ in the frequency domain. The problem is that the inverse filter typically has very high gain at certain frequencies so that the noise term completely dominates the result. One attempt to reduce the noise amplification is modify the inverse filter by weighing with a Butterworth response, in order to lower high-frequency gain.

$$T(u,v) = \frac{1}{1 + (\frac{u^2+v^2}{D^2})^n} H^{-1}(u,v) \tag{7}$$

It is not easy to weigh the inverse filter so that the image is not distorted and the noise is reduced. Wiener aims at minimizing Mean-Square-Error and is expressed in frequency domain as follows:

$$T(u,v) = \frac{H^*(u,v)}{|H(u,v)|^2 + S_\eta(u,v)/S_f(u,v)} \tag{8}$$

where $S_\eta(u,v)$ and $S_f(u,v)$ are the power spectra of the noise and the original image. For simplicity concern, this term can be substituted with a small positive integer, which leads to a Wiener approximation. The estimate of $S_f(u,v)$ is given by $\frac{S_g(u,v)-S_\eta(u,v)}{|H(u,v)|^2}$ or a small positive integer K. The Constrained Least-Square method seeks to constrain the variation in the image due to the noise without any knowledge or either power spectrum.

$$T(u,v) = \frac{H^*(u,v)}{|H(u,v)|^2 + \gamma|P(u,v)|^2} \tag{9}$$

where $P(u,v)$ is the Fourier transform the Laplacian filter.

For the evaluation of image denoising, we provides a comprehensive assessment system which consists of Peak Signal-to-Noise Ratio (PSNR), Weighted Peak Signal-to-Noise Ratio (WPSNR), Structural Similarity (SSIM) [3], and Mean-Square-Error (MSE). Let $\mathbf{x}$ and $\mathbf{y}$ denotes two images of size $W \times H$, the SSIM can be defined as:

$$SSIM(\mathbf{x},\mathbf{y}) = \frac{(2\mu_x\mu_y + c_1)(2\sigma_{xy} + c_2)}{(\mu_x^2 + \mu_y^2 + c_1)(\sigma_x^2 + \sigma_y^2 + c_2)} \tag{10}$$

where μ represent the mean value, σ denotes the deviation, c_1 and c_2 are two variables to stabilize the division with weak denominator. The MSE is calculated as:

$$MSE(\mathbf{x},\mathbf{y}) = \frac{1}{W \times H} \sum_{i=1}^{W} \sum_{j=1}^{H} (\mathbf{x}(i,j) - \mathbf{y}(i,j))^2 \tag{11}$$

Given the MSE, weighted MSE of an image and bit depth BD, the PSNR and WPSNR can be similarly defined as

$$\begin{aligned} PSNR &= 10\log_{10}(\frac{(2BD-1)^2}{MSE}) \\ WPSNR &= 10\log_{10}(\frac{(2BD-1)^2}{MSE_w}) \end{aligned} \tag{12}$$

2 System Description

All the codes are implemented in MATLAB 2019b. Additional library for calculating WPSNR is needed.

3 Results

3.1 Histogram Equalization

Fig. 1 shows differences between the original image ("Lena.bmp", 512×512, grayscale), a contrast-reduced version and the equalized version, with their respective histograms. The first histogram shows the distribution of gray-scale levels within the image and their corresponding occurrences (number of pixels).

After applying a function which reduces the dynamic range (contrast) of the image, we plot the histogram and we see that the pixels now take only values from around 51 to 95 (gray-scale level). Therefore, the range is restricted and the image does not exploit all possible information. From Shannon information theorem [4], we know that an equiprobable source contains the maximum entropy, thus we want to apply a transformation on the contrast-reduced image to make its probability density function as close as possible to uniform distribution. The histogram equalization is performed and shown in Fig. 1. We can observe now from the last histogram how the full range of gray-scale values is exploited and the corresponding image appearance of course has improved. Even though the result is not a flat uniform distribution, the transformation has helped spreading the histogram and enhanced image contrast.

This is because we deal with discrete values and not with an ideal continuous case (see Eq. 4). In particular, the probability values (occurrences) have not changed, as well as the number of bins, but only they have been mapped to a new the pixel bin value. Also small values of occurrence could disappear due to scaling and rounding operations.

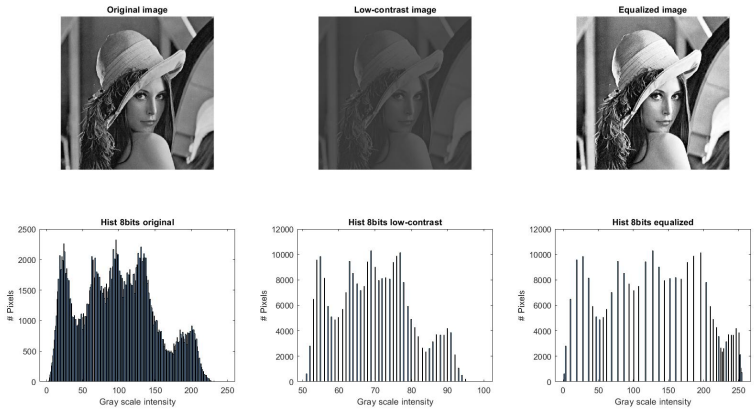

Figure 1: From left to right: original image, low-contrast image and equalized image, and corresponding histograms (bottom row).

3.2 Image Denoising

Fig. 2 displays visual effect of different noise and corresponding histogram. Salt-and-pepper noise add some outliers to the image, while Gaussian noise move some pixels into nearby bins in the histogram.

In Fig. 3 and Fig. 4, we present the result using mean and median filter applied on image with salt-and-pepper noise and Gaussian noise respectively. For the boundary pixels, we pad the image with mirror reflections. We summarize the quantitative analysis in Tab. 1. For salt-and-pepper noise, it is obvious that median filter provides a much smoother image and better approximates the original histogram. As for additive Gaussian noise, both filters achieve fair result, but mean filter slightly outperforms median filter. Median filter considers each pixel in the image at its nearby neighbors to decide whether or not it is representative of its surroundings. Instead of simply replacing the pixel value with the mean of neighboring pixel values, it chooses the median of neighborhood values. Since it is a non-linear filter, the shading/edges can possibly be preserved in the image, and it can effectively eliminate local extreme values such as salt noise. Mean filter is a kind of linear low-pass filter and outputs an average of each pixel's neighborhood, which can target additive zero-mean noise.

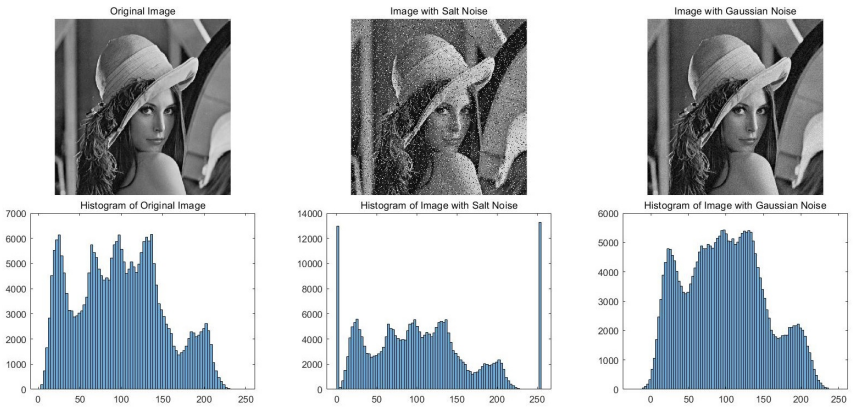

Figure 2: From left to right: original image, image with salt-and-pepper noise, image with Gaussian additive noise (top row), and corresponding histograms (bottom row).

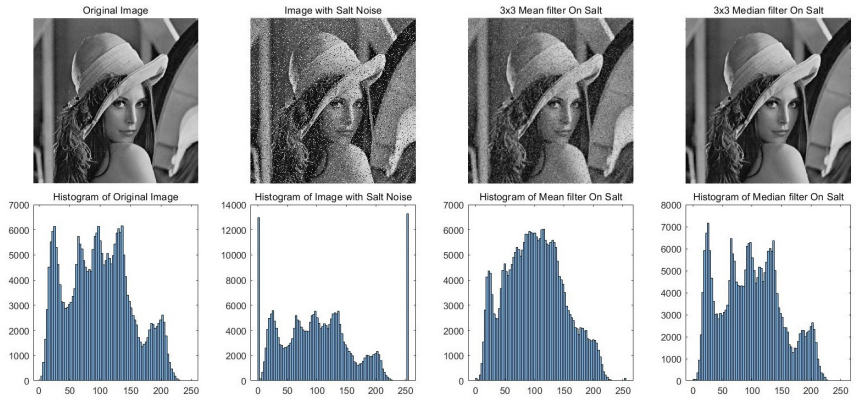

Figure 3: Mean and median filter applied on image with salt-and -pepper noise.

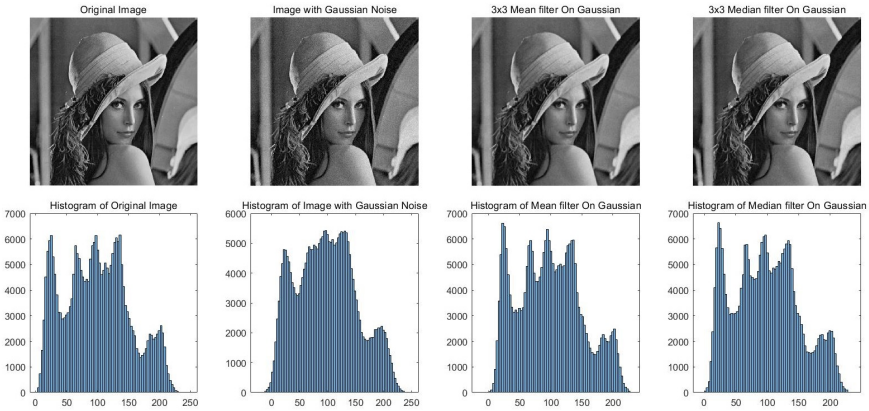

Figure 4: Mean and median filter applied on image with Gaussian noise.

Noise Source	Filter	PSNR↑	WPSNR↑	SSIM↑	MSE↓
Gaussian	Mean	31.44 dB	43.61 dB	**0.84**	**17.79**
Gaussian	Median	**31.85 dB**	43.95 dB	0.83	18.14
Gaussian	None	30.09 dB	**45.28 dB**	0.73	29.39
Salt-and-pepper	Mean	23.08 dB	31.07 dB	0.45	46.31
Salt-and-pepper	Median	**31.73 dB**	**44.32 dB**	**0.87**	13.58
Salt-and-pepper	None	15.17 dB	29.68 dB	0.19	**12.55**

Table 1: Quantitative comparison between median filter and mean filter on additive Gaussian noise and salt-and-pepper noise.

3.3 Frequency Domain Filtering

In this section we have explored four different types of frequency domain filters to restore a degraded image in order to observe strengths and weaknesses, namely: 1) Inverse filtering; 2) Modified Inverse filtering ; 3) Wiener filtering; 4) Constrained Least Squares filtering.

Fig. 5 shows the spectrum of original and degrade image. Lots of minor frequencies occur in the degraded image. It is worth to mention a large portion come from the loss in the edges (See also Fig. 5). In the convolution operation, we specify the command "same"to ensure the same image size. However, this will zero-pad the image so that the border is not well kept. The remedies can be either padding the image with mirror reflections or convolve the image without the boundary pixels taken into consideration. We visualize different boundary-keeping strategy, as shown in Fig. 6. As the matrix dimension of image and filter is not equal, we approximate wiener filter by substituting the ratio of power spectra with a small positive integer K. The hyper-parameter K for Wiener filter is set as 0.031, and γ for CLS filter is set 0.6 empirically after a trial-and-error method.

We present evaluation result for all filters in the Table. 2 and display the images in the Fig. 7 and Fig. 8. Note that the restored image is improved in terms of the visual and perceptual performance, but the quantitative evaluations do not indicate this. These metrics are not targeting deconvolution assessment.

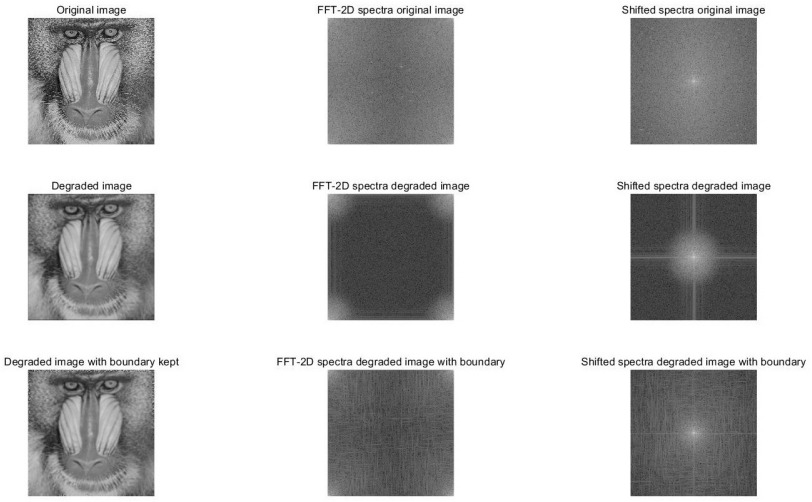

Figure 5: Original image in spatial and frequency domain (top row); degraded image in spatial and frequency domain (middle row); degraded image with boundary kept in spatial and frequency domain (bottom row).

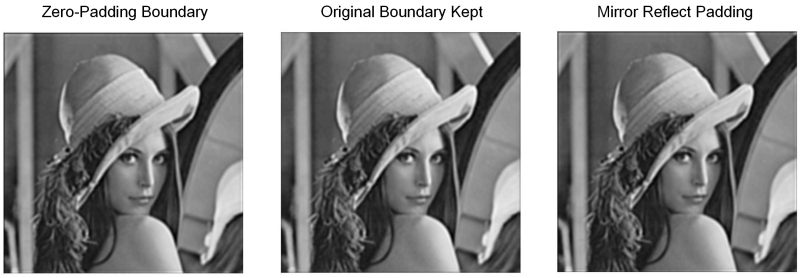

Figure 6: Restored image obtained by convolution using three boundary strategies: zero-padding, original boundary, and mirror reflection padding.

Approaches	**PSNR↑**	**WPSNR↑**	**SSIM↑**	**MSE↓**
Inverse Filtering	3.80 dB	9.82 dB	0.35	infinite
Modified Inverse Filtering	21.26 dB	27.38 dB	0.57	58.34
Wiener	24.25 dB	31.61 dB	0.73	51.48
Constrained LS	24.96 dB	32.41 dB	0.71	33.97
Degraded image	**26.49 dB**	**34.58 dB**	**0.75**	**30.02**

Table 2: Comparison of all restoration filters. The test image is Lena.

Figure 7: Restored image of Lena using different frequency filtering technique.

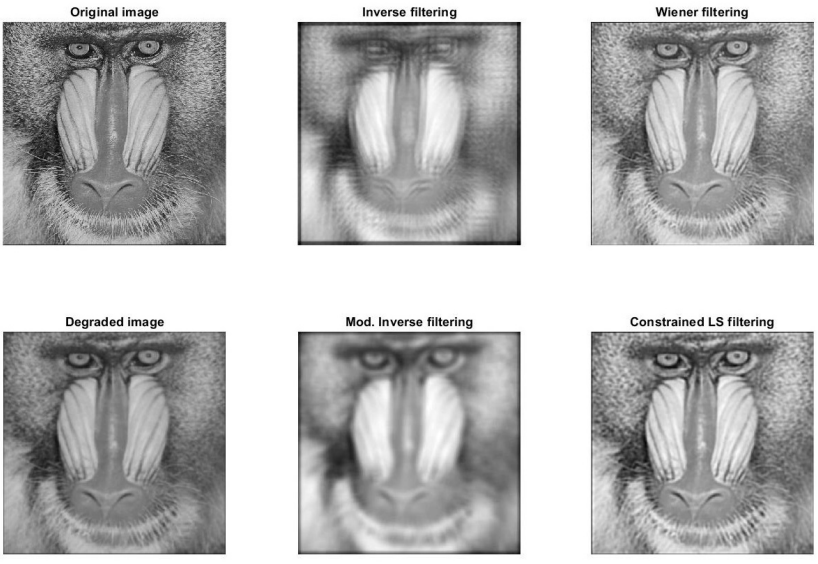

Figure 8: Restored image of Baboo using different frequency filtering technique.

4 Conclusions

In this project we have explored different techniques of image enhancement, both in spatial domain as point operations or filtering and in frequency domain. The most challenging part has been the frequency domain filtering because, although it provides easiness from an implementation perspective thanks to Fourier properties, the restoration filter was not trivial to implement not having a set of similar images to estimate a good power spectral density of the original image.

Appendix

Allocation of responsibilities

We divided the workload equally within the group. Federico implemented Histogram Equalization, Yue implemented Image Denoising, while challenges in Frequency Domain Filtering have been solved together.

References

[1] Rafael C. Gonzalez and Richard E. Woods, *Digital Image Processing*, Prentice Hall, 2nd ed., 2002

[2] M. Flierl. *Image and Video Processing [EQ2330], Course Slides, KTH, 2019*

[3] Wang, Zhou and Bovik, Alan C and Sheikh, Hamid R and Simoncelli, Eero P and others, *Image quality assessment: from error visibility to structural similarity*, IEEE transactions on image processing, Volume 13, 600-612, 2004

[4] Shannon Claude Elwood, *A mathematical theory of communication*, Bell system technical journal, Volume 27, 379-423, 1948